Supporting Information

Combining Nanostructuration with Boron Doping to Alter Sub-Bandgap Acceptor States in Diamond Materials

Sneha Choudhury, Benjamin Kiendl, Jian Ren, Fang Gao, Peter Knittel, Christoph Nebel, Amélie Venerosy, Hugues Girard, Jean-Charles Arnault, Anke Krueger, Karin Larsson, Tristan Petit**

Characterization of B-doped NDs

The milling of NDs was performed with a PULVERISETTE 23 (Fritsch, Germany) equipped with grinding bowl and balls (3 mm) made from tempered steel. After milling the ND particles still show the characteristic blueish color of the starting material, which is caused by the boron doping (see Fig. S1).

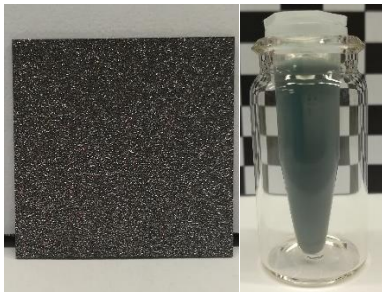

Fig. S1: B-doped starting material (left; 1.5 x 1.5 cm) and milled B-doped ND particles in aqueous dispersion (right; 1.5 ml with 1.0 wt%).

Parameters of the milling procedure, Zeta potential and hydrodynamic diameter (measured with a Zetasizer Nano, Malvern, UK) of the B:NDs in aqueous dispersion are shown in table S1.

Table S1: Amount of starting material, milling time, zeta-potential and hydrodynamic diameter measurements of 1.0 wt% aqueous dispersion of milled B-doped ND particles.

amount [mg]	milling time [h]	ζ [mV]	D-(10) [nm]	D-(50) [nm]	D-(90) [nm]
358	10	-41.0	147	664	942

In order to obtain different size fractions, a part of the whole sample (fraction I) was centrifuged (EBA 21 Typ 1004 benchtop centrifuge with fixed angle rotor, Hettich, Germany) at a specific speed and time (see table S2). The resulting fractions II and III were still slightly colored and showed a mean size of 50 nm (fraction II) and 30 nm (fraction III).

Table S2: Fractional centrifugation of B-doped ND particles.

fraction	centrifugation speed [rpm]	centrifugation time [min]	D-(10) [nm]	D-(50) [nm]	D-(90) [nm]
I	/	/	147	664	942
II	9000	5	34.9	50.7	80.1
III	15000	10	21.7	33.4	59.3

In Fig. S2 SEM images of the starting material and fraction I, recorded with an Ultra Plus field emission scanning electron microscope equipped with a GEMINI e-Beam column operated at 4.00 kV (Zeiss, Germany) are shown. The microcrystalline starting material has single grains measuring up to 100 µm. Fraction I, the whole milled B-ND sample, contains all kinds of particle size. From the smallest particles ~ 25 nm up to still micrometer sized particles. The non-nanometer material can be isolated via centrifugation and be milled a second time to obtain an all-nanometer sample.

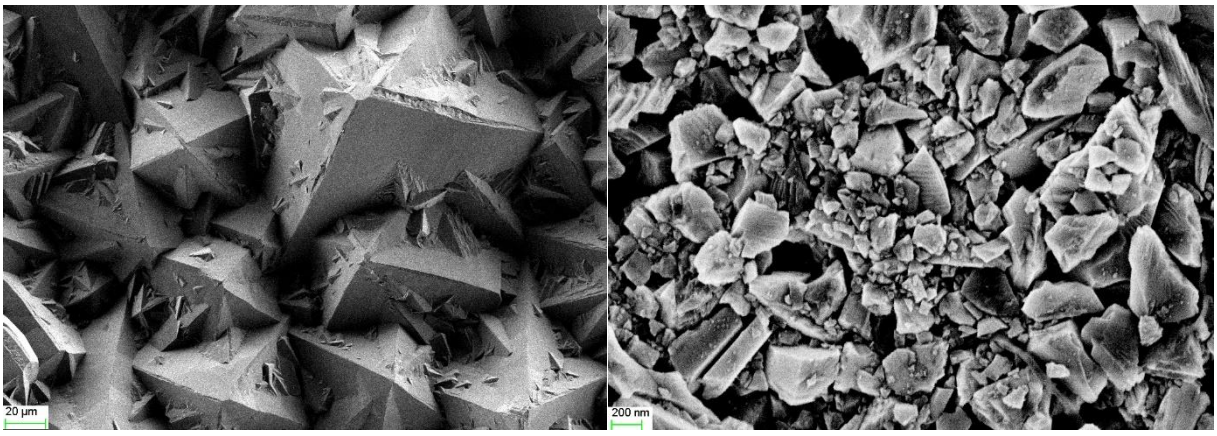

Fig. S2: SEM picture of the starting material (left) and fraction I (right).

When looking at the fractions II and III, the results obtained by DLS are in good accordance with the crystallite size determined via SEM (see Fig. S3). For fraction II, the mean crystallite size was 48 nm, with the largest particles being ~85 nm and the smallest ones ~28 nm. For fraction III, the mean size was 33 nm, with the largest particles being ~61 nm and the smallest ones ~18 nm.

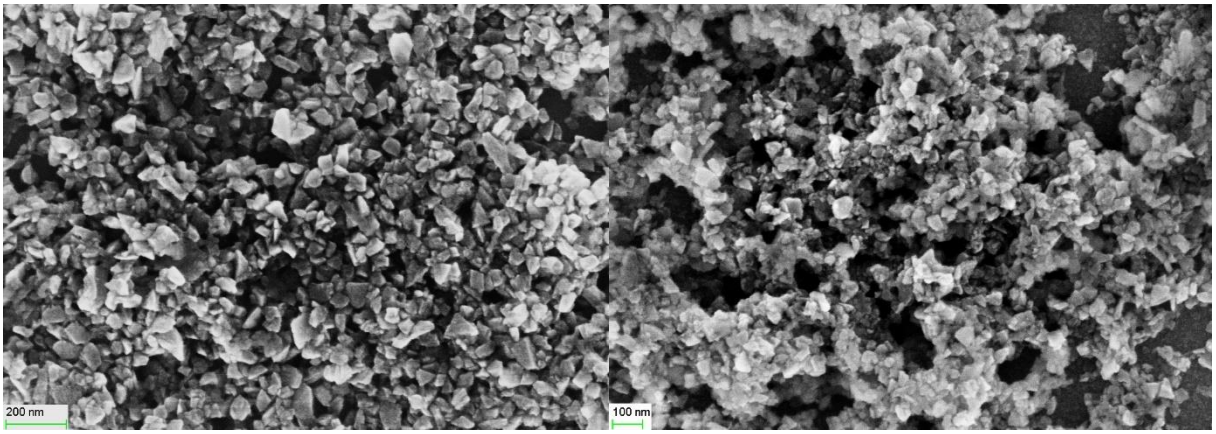

Fig. S3: SEM picture of fraction II (left) and fraction III (right).

The Raman spectra (DXR Raman microscope, Thermo, UK) show also some interesting features (see Fig. S4). When measuring the front side of the starting material, just a very sharp peak at 1329 cm^{-1} related to sp^3-bonded carbon is visible. In contrast, the back side shows the Fano resonance at ~499 cm^{-1} and another band at ~1228 cm^{-1}, both confirm boron doping above 10^{20} atoms/cm^{-3}. SIMS measurements proved that the boron concentration of the starting material is ~2.2 x 10^{20} atoms/cm^{-3}. The quite intensive G-band at 1543 cm^{-1} must have its origin in the removing process of the silicon substrate. None of the obtained B-doped ND particle fractions show significant boron signals. Next to the diamond signal at 1329 cm^{-1} a G-band is visible at ~1537 cm^{-1}, which can be explained by the high density of sp^2-containing grain boundaries coming to surface after milling. The missing of any boron signal is due to loss of boron during the milling. The concentration is found to be around 1.8 x 10^{20} atoms/cm^{-3} (1020 ppm) as measured by Elemental Analysis technique.

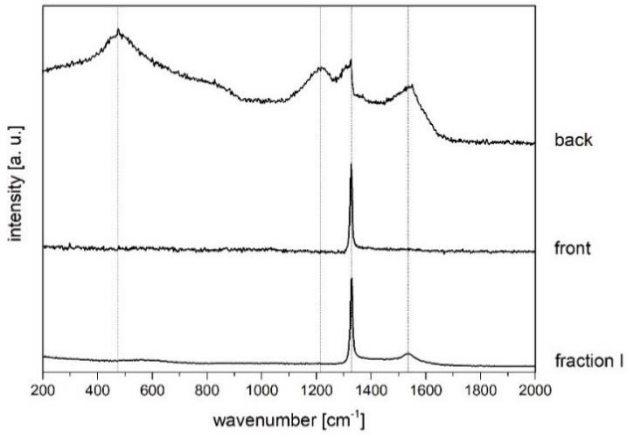

Fig. S4: Raman spectra of B-doped ND particles (fraction I) and B-doped starting material from back and front side (excitation at 445 nm).

pDOS of B-doped diamond (111) surfaces

In the present investigation, a super cell model for the non-terminated (111) diamond surface plan was also constructed which is presented in the figure below.

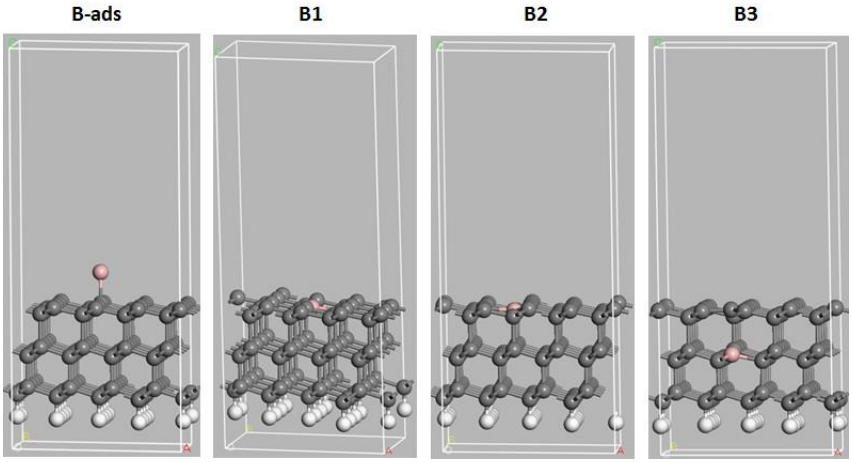

Fig. S5: Super cells showing the different non terminated (111) diamond surfaces, with B positioned as adsorbed (B-ads) or in atomic layer 1 (B1), 2 (B2), or 3 (B3), respectively. C, H and B are shown in grey, white, and pink, respectively.

The partial density of states (pDOS) for the H-terminated, non-terminated and Pandey Chain reconstructed (111) diamond surfaces for different boron carbon co-ordinations are shown in the figures below.

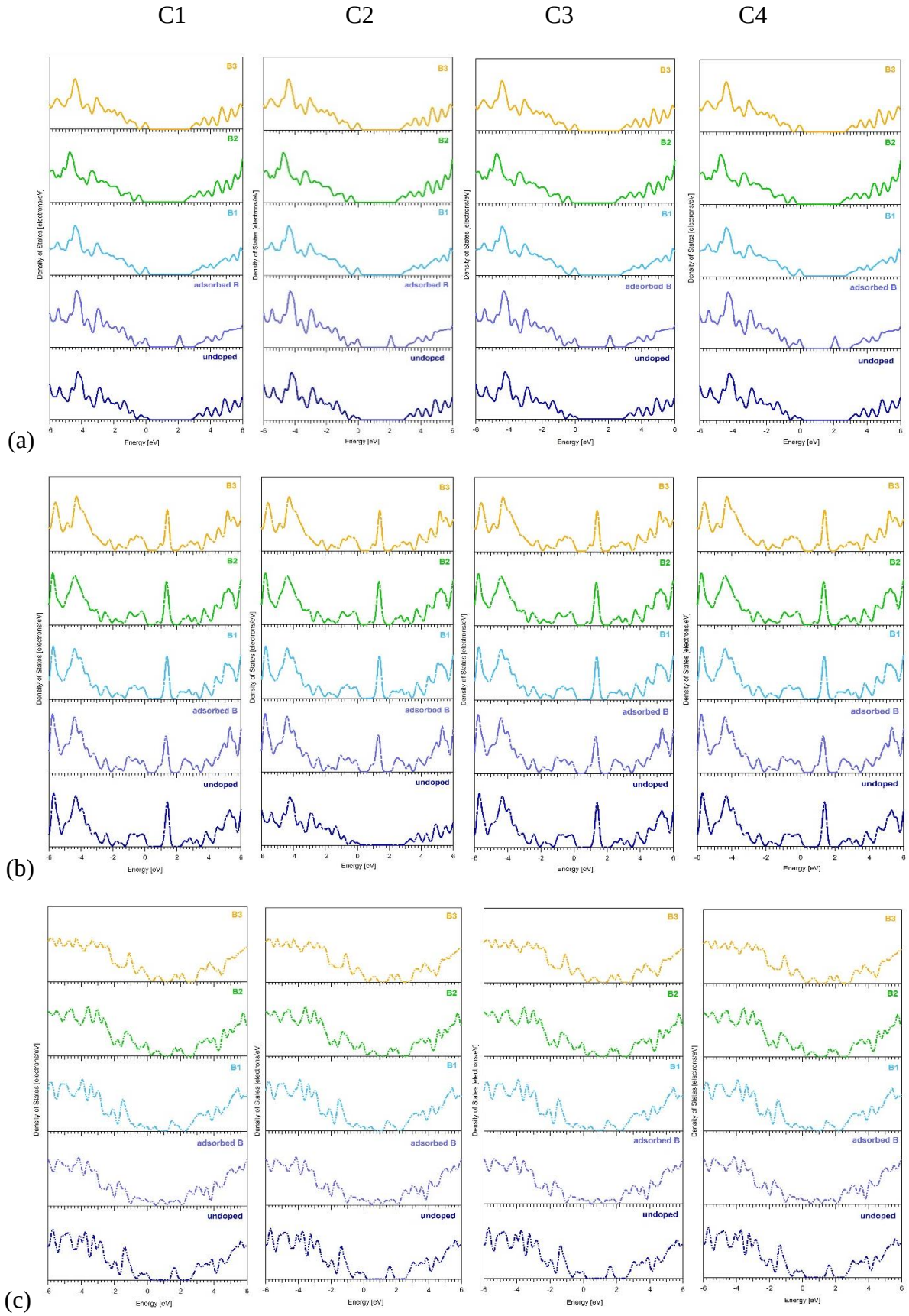

Fig. S6: pDOS of carbon at (a) H-terminated, (b) non-terminated and (c) Pandey chain reconstructed (111) diamond surfaces with different B positions in the top (C1), second (C2), third (C3) and foruth (C4) carbon layers in the lattice

Electron Affinity of the Investigated Diamond Surfaces

The electron affinity (EA) values of B-doped diamond (111) surfaces as shown in Table S3 were estimated by using the following equation:

$EA = E_{zero} – (E_{VBE} - E_{bandgap})$

where E_{VBE} and $E_{bandgap}$ are the energy of valence band edge and bandgap respectively. E_{zero} is the level of 0 eV, where the electrons are not bonded to the surface.

Table S3: Electron Affinity values of the different B-doped diamond (111) surfaces with different positions of the boron atoms as determined by DFT calculations

	H-terminated (in eV)	**Pandey-Chain Reconstructed (in eV)**	**Non-terminated (in eV)**
Non-doped	-1.1	-1.4	-1.8
B-ads	1.0	-1.2	-1.5
B1	-0.4	-1.4	-1.7
B2	-1.3	-1.2	-1.6
B3	-1.4	1.0	-1.5